Title

Exhaled breath condensate profiles of U.S. Navy divers following prolonged hyperbaric oxygen (HBO) and nitrogen-oxygen (Nitrox) chamber exposures

Journal

Journal of Breath Research, 17(3)

ISSN

1752-7155

Authors

Fothergill, David M

Borras, Eva

McCartney, Mitchell M

et al.

Publication Date

2023-07-01

DOI

10.1088/1752-7163/acd715

HHS Public Access

Author manuscript

J Breath Res. Author manuscript; available in PMC 2024 April 29.

Published in final edited form as:

J Breath Res. ; 17(3): . doi:10.1088/1752-7163/acd715.

Exhaled breath condensate profiles of US Navy divers following prolonged hyperbaric oxygen (HBO) and nitrogen-oxygen (Nitrox) chamber exposures

David M. Fothergill[1,*], **Eva Borras**[2,3], **Mitchell M. McCartney**[2,3,4], **Edward Schelegle**[5], **Cristina E. Davis**[2,3,4]

[1]Naval Submarine Medical Research Laboratory, Groton, CT

[2]Mechanical and Aerospace Engineering, One Shields Avenue, University of California, Davis, Davis, California, USA

[3]UC Davis Lung Center, One Shields Avenue, University of California, Davis, Davis, California, USA

[4]VA Northern California Health Care System, Mather, California, USA

[5]Department of Anatomy, Physiology, and Cell Biology, School of Veterinary Medicine, University of California, Davis, Davis, California, USA

Abstract

Prolonged exposure to hyperbaric hyperoxia can lead to pulmonary oxygen toxicity (PO2tox). PO2tox is a mission limiting factor for special operations forces divers using closed-circuit rebreathing apparatus and a potential side effect for patients undergoing hyperbaric oxygen (HBO) treatment. In this study, we aim to determine if there is a specific breath profile of compounds in exhaled breath condensate (EBC) that is indicative of the early stages of pulmonary hyperoxic stress/PO2tox.

Using a double-blind, randomized “sham” controlled, cross-over design 14 U.S. Navy trained diver volunteers breathed two different gas mixtures at an ambient pressure of 2 ATA (33 fsw, 10 msw) for 6.5 hours. One test gas consisted of 100% O2 (HBO) and the other was a gas mixture containing 30.6% O2 with the balance N2 (Nitrox). The high O2 stress dive (HBO) and low O2 stress dive (nitrox) were separated by at least seven days and were conducted dry and at rest inside a hyperbaric chamber. EBC samples were taken immediately before and after each dive and subsequently underwent a targeted and untargeted metabolomics analysis using liquid chromatography coupled to mass spectrometry (LC-MS).

[*]Corresponding author: Dr. David Fothergill (david.m.fothergill.civ@health.mil).

Disclaimer

The views expressed in this article reflect the results of research conducted by the authors and do not necessarily reflect the official policy or position of the Department of the Navy, Department of Defense, nor the U.S. Government. The study protocol (NSMRL.2017.0002) was approved by the Naval Submarine Medical Research Laboratory Institutional Review Board in compliance with all applicable Federal regulations governing the protection of human subjects. Dr. David Fothergill is an employee of the U.S. Government. This work was prepared as part of his official duties. Title 17 U.S.C. §105 provides that ‘Copyright protection under this title is not available for any work of the United States Government.’ Title 17 U.S.C. §101 defines a U.S. Government work as a work prepared by a military service member or employee of the U.S. Government as part of that person’s official duties.

Following the HBO dive, 10 out of 14 subjects reported symptoms of the early stages of PO2tox and one subject terminated the dive early due to severe symptoms of PO2tox. No symptoms of PO2tox were reported following the nitrox dive. A Partial Least-Squares Discriminant Analysis of the normalized (relative to pre-dive) untargeted data gave good classification abilities between the HBO and nitrox EBC with an AUC of 0.99 (± 2%) and sensitivity and specificity of 0.93 (± 10%) and 0.94 (± 10%), respectively. The resulting classifications identified specific biomarkers that included human metabolites and lipids and their derivatives from different metabolic pathways that may explain metabolomic changes resulting from prolonged HBO exposure.

Keywords

pulmonary hyperoxic stress; breath analysis; metabolomics; oxygen toxicity

1. Introduction

Although oxygen is needed to sustain life, breathing higher than normal partial pressures of oxygen for prolonged periods of time results in pulmonary oxidative stress that can reduce lung function and lead to pulmonary oxygen toxicity (PO2tox). Pulmonary oxygen toxicity can be a mission limiting factor for professional and military divers breathing on closed circuit rebreathers or mixed gas breathing systems (1). It is also a potential side effect of hyperbaric oxygen treatment that is currently accepted for use for 14 medical conditions (2), as well as with normobaric oxygen administration for acute respiratory distress syndrome.

The time of onset of PO2tox depends on the partial pressure of the oxygen breathed, the duration of the oxygen exposure, and the individual's susceptibility to pulmonary toxicity. Typical early symptoms of PO2tox include, dry or itchy cough, substernal tickling, chest tightness and difficulty inspiring, or lung pain during inspiration from the oxygen-induced tracheobronchitis. These symptoms may also induce a sensation of dyspnea especially during exercise. If an individual breathes high levels of oxygen for too long this can lead to pulmonary edema because of interstitial fluid accumulation.

Objective assessments of the early stages of PO2tox have traditionally relied on pulmonary function testing such as vital capacity (VC), forced VC (FVC), force expiratory volume in 1.0 second (FEV1), and the diffusion capacity of the lungs for carbon monoxide (DLCO). However, these traditional pulmonary function tests show high between subject variability in the magnitude of the observed changes following a given oxygen exposure and are often unrelated to the symptomology reported, with some subjects showing significant decrements in lung function without reporting any symptomology while others who report symptoms of PO2tox often able to produce normal spirometry values (3) (4). Given the above limitations of traditional pulmonary function testing to detect the early signs of PO2tox, alternative assessments are needed that are both sensitive and specific to the biochemical changes that occur with prolonged hyperoxic exposures. Examination of the biomarkers contained in the exhaled breath condensate may offer a solution for the early detection of PO2tox.

Exhaled breath condensate (EBC) has been increasingly used as a novel method to study airway inflammation for a variety of pulmonary diseases such as asthma, cystic fibrosis,

chronic obstructive pulmonary disease, and interstitial lung diseases (5–8). Furthermore, metabolomic patterns in EBC have been found to differ between healthy, inflammatory, and infectious airways (9–11). As EBC is easy to collect, non-invasive, and effort independent (unlike spirometry which requires repeated maximum breathing efforts), biomarkers found in the EBC may provide a more sensitive and reliable non-invasive test of PO2tox that can detect pulmonary oxidative stress at an earlier stage in the toxicity process than traditional pulmonary function tests. In this study, we aim to determine if there is a specific breath profile of compounds in EBC that is indicative of the early stages of pulmonary hyperoxic stress/oxygen toxicity. A secondary aim is to compare the EBC metabolomic profile following a prolonged hyperbaric oxygen dive to that following a prolonged hyperbaric nitrogen-oxygen dive to identify the separate effects of oxidative versus decompression stress on biomarkers in the EBC.

2. Material and Methods

2.1. Study design

The study was a double blind randomized “sham” controlled cross-over design in which subjects breathed two different gas mixtures at an ambient pressure of 2 ATA (33 fsw, 10 msw) for 6.5 hours. The hyperbaric exposures were conducted dry and at rest inside a hyperbaric chamber. One test gas consisted of 100% O2 (HBO) and the other was a gas mixture containing 30.6% O2 with the balance N2 (Nitrox). The test gases were administered to the subjects using Scott oral nasal masks connected to the chamber’s built-in breathing system and were designed to differ significantly in the level of hyperoxic stress presented to the subjects. Based upon previous work (4) the 2 ATA inspired partial pressure of oxygen (PiO2) administered during the HBO dive was predicted to result in observable signs and symptoms of pulmonary oxygen toxicity in approximately half of the subject population following 6.5 hours of exposure. In contrast, the much lower PiO2 of the nitrox gas mixture (PiO2 = 0.61 ATA) was intended to act as a “sham” or control dive in which the pulmonary hyperoxic stress was significantly below that of the HBO, and not expected to result in any signs or symptoms of pulmonary oxygen toxicity after 6.5 h of exposure. The PiO2 chosen for the nitrox dive also allowed the depth-time profile of the nitrox dive to match the 6.5 h HBO dive exposure.

2.2. Subjects

Fourteen male U.S. Navy trained divers volunteered to participate in the study. The average and standard deviation (mean±SD) age and weight were 33.1 ± 7.5 years and 84.3 ± 11.8 kg, respectively. All subjects were informed of the risks of the study and signed an informed consent. As one of the primary risks of the study was oxygen toxicity they were briefed on the signs and symptoms of central nervous system and pulmonary oxygen toxicity and asked to report any onset of symptoms to the inside dive tender. All the subjects were followed up 24 h and 48 h after each dive to ensure they had full recovery of pulmonary function and symptomology. Furthermore, each diver was medical evaluated by a diving physician (who was independent of the study) on the morning prior to conducting each dive to ensure they were fit and healthy and cleared to dive. Additionally, each diver was debriefed after each dive by the principal investigator for any signs or symptoms relating to pulmonary oxygen

toxicity that they currently had or had experienced during the dive. The dive exposures were conducted in teams of two or three subjects exposed to the test gas in the chamber at the same time.

2.3. Breath sampling

EBC samples were collected using a custom EBC sampler device described by Valenzuela and Encina (12). The device included a Hans Rudolph breathing valve with mouthpiece and spit trap with two Tygon capillary lines connected to the exhalation port of the breathing valve. The two capillary lines were attached to a double set of glass vials which were immersed in ice to condense and collect the EBC (Figure 1). Immediately before and after each dive the subjects performed 15 min of normal tidal breathing wearing a nose piece. After each collection, the EBC vials were retrieved from the tubes and stored at −80 °C until analysis. A minimum amount of 200 uL was collected through all the vials for each sample.

2.4. Sample preparation

Each EBC sample was thawed, and the maximum available volume was aliquoted in 2 mL glass amber vials. When volumes did not reach 250 uL on different vials from the same sample, these were merged in a common sample; if the volume was higher than 250 uL then, those samples were considered duplicates. A mixture of internal standards (IS, mixture of deuterated oxylipins) and antioxidant solution (butylated hydroxytoluene (BHT) and EDTA at 0.2 mg/mL, each in a solution of methanol:water (1:1)) were added to each EBC sample. Samples were then mixed and frozen for 30–60 min at −80°C to remove water content and provide lyophilized samples for analysis. Dried extracts were reconstituted using 60 μL of mobile phase (95% water in acetonitrile), and then vortexed and sonicated for 10 min at 4°C. Reconstituted samples were finally centrifuged at 13,000 rpm for 10 min at 4°C and the supernatant was stored at −80°C until LC-MS analysis.

Simultaneously, quality controls (QCs) and blanks (QC blanks) were prepared by pooling EBC and adding known concentrations of oxylipin standard mix following the same preparation process for all the samples. Names, molecular formulas, exact masses, LC-MS retention times, and preferred precursor ions used for MS/MS data of the targeted compounds are described elsewhere (data showed in supplementary Table S1 (7)). The targeted compounds were those mainly related to inflammation and oxidative stress, from pathways such as cyclooxygenase (e.g., prostaglandins and thromboxanes), lipoxygenase (e.g., 5-, 12-, 15-HETE, leukotrienes, DiHETEs, HEPE, etc.), and cytochrome P450 (e.g., HETEs, EETs, DiHOMEs, etc.).

2.5. Sample analysis

An Agilent 1290 series HPLC system coupled with an Agilent 6530 quadrupole-time of flight (qTOF) mass spectrometer (Agilent Technologies, Santa Clara, CA, USA) was used to analyze all samples. Samples were injected (20 uL) using an autosampler at 5°C into an InfinityLab Poroshell 120 EC-C18 column (3.0 mm × 50 mm, 2.7 μm) (Agilent Technologies, Palo Alto, CA, US) held at 35°C. Compounds were separated at a flow rate of 600 μL/min using solvent gradient of water (A) and acetonitrile (B), both with 0.1% formic acid. Electrospray ionization (ESI) was achieved with an Agilent Jet Stream nebulizer, and

samples were run twice, one in positive and one in negative ESI mode. Fragmentor voltage was set at 130 V and ionization was performed at 250°C using 3000(+)/4000(–) V. Mass ranges were set up from 60 to 1000 and from 100 to 970 m/z for positive and negative, respectively, with a scan rate of 2 spectra/s. Agilent reference masses were used to calibrate the system, using m/z 121.0508 and 922.0098 in positive mode, and m/z 119.0363 and 966.0007 in negative mode. In both modes, all ion fragmentation (MS/MS) was performed at collision energies of 0 and 15 V.

2.6. Data analysis

Targeted, and untargeted strategies were both used to analyze data acquired in negative mode. Positive mode data was treated for untargeted purposes. Raw data was initially checked with Agilent's Mass Hunter Qualitative Analysis B.06.00 software for qualitative reasons.

Agilent's Mass Hunter Quantitative (qTOF) Analysis B.07.00 software was used for targeted purposes, where compounds were identified, confirmed, and integrated using accurate mass, retention time, and MS/MS information. Quantification was preformed using standard calibration curves with internal standard corrections. QCs were used to validate the calibrations. Agilent's Mass Hunter Profinder B.08.00 Mass Profiler Professional (MPP, V13.0) software was used for untargeted analysis. Raw data were deconvoluted and obtained peaks were aligned and integrated using 30 ppm and 0.025 Da mass tolerance and a retention time window of 0.3 min. This process provides a peak table with samples in columns and variables or features in rows, containing peak areas or intensities.

All samples were randomly injected into the LC-MS. Raw peak tables were first cleaned by removing features that: appeared in blank samples with signals higher than 10 (peak sample/blank ratio), were missing in more than 50% of samples, had low repeatability (Relative Standard Deviation (RSD) > 25% in the QC pooled samples), and had near-constant values (RSD < 5% in all samples). To remove systematic bias between measures, samples were normalized using the original sample volume used per each sample. All missing values were replaced by the Limit of Detection (LOD)/5 or by minimum positive value divided by 5, in targeted and untargeted data, respectively. Heteroscedasticity was corrected in the final datasets using log transformations (13). Untargeted analyses were performed considering positive and negative modes in a merged dataset.

Excel, MATLAB R2017a, and PLS Toolbox V8.6.2 software were used for univariate and multivariate analyses. Parametric and non-parametric tests (t-tests/Wilcoxon rank sum test, or ANOVA/One-way Kruskal-Wallis test) were used to compare means and assess the significance of the fold change (FC) for the various compounds observed. FC and p-values were combined using Volcano Plots, allowing an initial variable selection by detecting features that explain significant differences. Fold change higher than two and false discovery rate adjusted p-values < 0.05 (Benjamini-Hochberg correction) were used as a criterion for selecting features. Subsequently, the following multivariate models were used for comparative analyses: principal component analysis (PCA), hierarchical cluster analysis (HCA), and Partial Least-Squares Discriminant Analysis (PLS-DA). PCA was performed initially to visualize similarities between observations and detect potential outliers in an

unsupervised way. PCA projects the maximum variance of the dataset in a linear additive model. Principal components (PC) are orthogonal variables that rank variances of features and reduce the dimensionality of the multivariate data set. HCA aims to group together data using a repeated calculation of distance measures between objects. Finally, PLS-DA was used as a classification method, with a supervised approach. It used correlation between the dataset of features and a matrix of known responses that contain sample information and classes/groups. PLS-DA provided different groups of samples based on their features (14, 15). Classification ability was determined by sensitivity (probability of correctly detecting a class), specificity (ability to reject a class), and area under the curve (AUC) values, which were defined by receiver operating characteristic (ROC) curves. AUC measures the classification ability at different thresholds, telling how much a model is able to distinguish classes or groups (16). PLS-DA also provided a list of potential markers related to a defined class ranked by variable importance in projection (VIP) values. VIPs summarized the impact of each feature in the model and values higher than 0.9 were considered relevant for that classification (17). Identifications of these relevant features or potential markers were performed by searching through a commercial database (METLIN) and using measured accurate masses to calculate a molecular formula and characterize each marker. Identifications were putatively reported when experimental and theoretical spectral pattern (scores) of the compounds were higher than 65%.

The effects of hyperbaric oxidative stress were analyzed by comparing the EBC metabolic profiles measured before and after the HBO dive, while the impact of the decompression stress was analyzed by comparing the nitrox pre and post EBC profiles as well as the post-dive HBO and nitrox EBC samples to each other.

3. Results and discussion

3.1. Symptomology

During the nitrox dive, none of the subjects reported any symptoms of pulmonary oxygen toxicity. During the HBO dive, one subject (subject 8) reported symptoms of dry cough 3 hours into the dive that continued to worsen over the next couple of hours. At 4.5 hours into the dive, that subject reported breathing discomfort and difficulty taking a full inspiration. Following a medical evaluation in the chamber, the subject was decompressed to the surface after a total time of 304 min on O2. This subject was the only subject with severe signs and symptoms of pulmonary oxygen toxicity that resulted in early termination of the HBO dive. Three subjects reported moderate symptoms of pulmonary oxygen toxicity following the HBO dive that included: “burning irritation in the chest, sensations of the need to cough, feeling out of breath, or the inability to take a deep breath.” Six subjects had relatively mild symptoms of pulmonary oxygen toxicity (e.g., minor discomfort on inhalation) and four subjects reported that they did not experience any symptoms of pulmonary oxygen toxicity following the O2 dive.

3.2. Effects on the EBC metabolic profile

Targeted analysis showed low concentrations of the compounds of interest, being closer to the limit of detection (LOD) defined by the method. Only 18 compounds out of 55

showed enough concentrations above LOD on more than 50% of the samples. Raw data for untargeted analysis contained 3431 and 6856 features for negative and positive modes, respectively. Features were cleaned as described previously, and both ionization modes were merged, leading to a dataset with 66 samples (including duplicates of some samples) and 5030 variables (features). Different normalization procedures were tested (sample volume, internal standard, median, and sum), and samples normalized by the volume of EBC used in initial preparation provided the best results.

Prior to discussing the results of the targeted oxylipin analysis performed in this study it is important to recognize the limitations in interpreting the changes seen in the concentrations of the oxylipins identified. First, while representing constituents of airway lining fluid contained in the exhaled breath condensate, they are diluted with condensed water vapor from the respiratory tract. In addition, this dilution can vary considerably from 200:1 to 2000:1 (18). This dilution can affect those compounds that are above the level of detection, which is not necessarily indicative of its biologic effect. Second, though present in the lung, the oxylipins identified may not be produced in the lungs but may have a systemic origin. While we can describe the metabolic pathways involved in their production and potential biological effects, we cannot use the changes in the observed oxylipins as a marker of any specific response in this study.

a) Effect of the hyperbaric oxygen (HBO) exposure.—Initial analysis of EBC targeted compounds detected from the O2 dive showed low classification abilities and high variabilities between pre and post exposures with the PLS-DA model showing an AUC of 0.55±30%, indicating a classification ability that is no better than chance. The high variability (±RSD%) is defined by 50 iterations splitting datasets using 33% of samples randomly as prediction/test sets. High RSDs showed low reliability for the results obtained in this classification model. However, we can observe the predicted ability to define samples as pre or post exposure in Figure 2a and relevant compounds (i.e., 19-HETE, 5-HEPE, PGJ2, 11(12)-DiHET and 9(10)-EpOME) that show more significant variation before and after the HBO dives (Figure 2b).

Of the five identified oxylipins shown in Figure 2b, two increased (19-HETE and 5-HEPE) and three decreased (PGJ2, 11(12)-DiHET, and 9(10)-EpOME) with hyperbaric hyperoxia. 19-HETE is a major cytochrome P450 2Js metabolite of arachidonic acid in multiple tissues, including liver, cortex, respiratory and olfactory mucosa, heart, bronchi, lung, spleen, small intestine, and kidney (19). It is also a potent vasodilator of the afferent arterioles in the kidney (20) and a potent stimulator of the sodium-potassium ATPase in the thick ascending limp of the loop of Henle in the kidney (21), increasing sodium and water reabsorption. 5-HEPE is an anti-inflammatory lipoxygenase metabolite of eicosapentaenoic acid that has been shown to induce the migration of regulatory T lymphocytes in adipose tissue (22).

Prostaglandin J2 (PGJ2), 11(12)-DiHET, and 9(10)-EpOME decreased with hyperbaric hyperoxia. PGJ2 is formed from PGD2 by spontaneous dehydration (23) and is an agonist of the prostaglandin D2(PGD2) receptor subtypes DP1 and DP2/CRTH (24) (25). In HEK293 cells expressing the human DP1 and DP2/CRTH receptors, PGJ2 increases or inhibits the production of cAMP, respectively (24, 25). PGJ2 is neurotoxic and induces

apoptosis, oxidative stress, and the accumulation of ubiquitinated proteins in the brain. 11(12)-DiHET is a cytochrome P450-monooxygenase system metabolite of arachidonic acid that has been shown to increase immediately and 24 hours after hyperbaric hyperoxia in rats (26), though it decreased following our hyperoxic exposure study. 11(12)-DiHET produces vasorelaxation in isolated porcine coronary artery rings precontracted with a thromboxane mimetic (27). 9(10)-EpOME, also known as leukotoxin, is a cytochrome P450 2C9 metabolite of linoleic acid in pulmonary endothelial cells and other cell types. 9(10)-EpOME induces oxidative stress and neutrophil chemotaxis (28, 29). Oxylipins have a wide range of functions, including apoptosis, tissue repair, blood clotting, cell proliferation, blood vessel permeability, pain, inflammation, immune actions, and blood pressure regulation, however, many of their functions are still being elucidated. Thus, the observed changes in the concentrations of the aforementioned five oxylipins following the HBO dive requires further study to elucidate their significance as biomarkers of the body's response to hyperoxic stress.

When looking at untargeted data, the effect of 6.5h HBO exposure at 2 ATA achieved high classification abilities, with AUC values close to one (0.92±9%), sensitivity of 0.78(±26%) and specificity of 0.92 (± 13%). A PLS-DA scores plot using all subjects is presented in Figure 3a, showing differentiated classes from EBC samples obtained before (pre) and after (post) the HBO dive. Lower sensitivities were explained by higher variability on the post-dive, mainly due to a single "post" sample (Subject 05) that was outside the confidence limit, showing high Hotelling T2 and Q residual values (Figure 3a). After deleting this outlier (as well as the pre value for subject 5), the new model achieved an AUC of 0.98 (± 4%) and sensitivities and specificities of 0.88 both (<±25%) (see PLS-DA scores plot shown in Figure 3b). When predicted values (Y pred) were calculated for this model, we observed that most of the samples were correctly classified based on "pre" and "post" dives (boxplot, Figure 3c), showing good predictability of this model. In this case, samples within "pre" subjects are more diverse, being more similar than the "post" samples within its own group. Interestingly, one of the "pre" samples, that of subject 8 shown in Figure 3b, was consistently misclassified as "post". This subject was the only subject who showed severe symptoms of pulmonary oxygen toxicity that resulted in early termination of the HBO dive. While the "post" sample data point for subject 8 did not differ markedly from the HBO post-dive group data, the fact that subject 8's pre-dive EBC profile appeared close to that observed post-dive could be related to this individual's particular sensitivity to PO2tox.

PLS-DA models also allowed the determination of certain characteristic features or compounds that explain the differences between pre- and post-dive EBC for the HBO experiment. The PLS-DA model was built using 141 selected variables related to differences between exposures. From these initial 141 variables, 54 features had high VIP values (VIP >0.9). Approximately half of the features (48%) were identified with scores higher than 65%. Table 1 describes 26 of these characterized features, which have been defined with molecular formula, putative compound identification, a score value (%) by comparing spectra to METLIN database, up- or down-regulation after the HBO dive, and a short description of the compound. An expanded list of the 54 tentatively identified compounds with VIP values >0.9 together with their ID scores, log fold change between pre and post HBO, and p values, is provided in supplemental Table S2. Out of the 54 features,

most showed a decrease in intensity after the 6.5h HBO exposure at 2 ATA. Only 24% of the features were up-regulated. The majority of the compounds are described as potential human metabolites and fatty acyls that come from different metabolic pathways, such as derivatives of eicosanoids and oxylipins from cyclooxygenase (COX), lipogenase (LOX), cytochrome P450 and other non-enzymatic pathways. Some drug metabolites were identified (e.g., hydroxytetrabenazine/eucaine or dihydroergocryptine) but with low ID scores (<85%). With high ID scores we identified eicosanoids like hydroxyeicosatetraenoic (DiHETE) or hydroperoxyeicosatetraenoic (HpETE) acids, and fatty acids like 3-hydroxy-tetradecanedioic acid. This later compound was detected in positive and negative mode simultaneously, showing a reduction in its intensity after the HBO dive. An alkane containing 6 carbons (compound 5 Table 1) was also down-regulated. Although high ID score values were achieved, it was difficult to characterize many of the features, which shared formula and mass spectra with several compounds (see Supplemental Table S2).

To determine if the EBC breath pattern of the 10 subjects who reported PO2tox symptoms following the HBO exposure were different from the four subjects who did not have any PO2tox symptoms, an additional PLS-DA model was developed in which the normalized HBO EBC data (log intensity post dive/log intensity pre-dive) was analyzed and classified according to presence/absence of symptoms. As shown in Figure 4 this PLS-DA model achieved a good ability to classify the HBO dive EBC samples according to the presence or absence of symptoms ($p = 2.7e-7$) with an AUC of 1 (±1%), specificity of 0.94 (±15%), and sensitivity of 0.88 (±37%). This PLS-DA model was comprised of 127 selected variables, 42 of which had high VIP values (>0.9) and 18 of which were characterized with high ID score values (>65%). Table 2 shows putative identifications and molecular formulas, METLIN database-based score value (%), up- or down-regulation by symptomology relative to pre-dive HBO conditions, and a short description of the compounds. Most of the features (88%) were up-regulated, meaning their intensities were higher when symptoms showed up in subjects after the 6.5h HBO exposure at 2 ATA. Those down-regulated features in Table 2 represent compounds that were more highly expressed when no symptoms were detected after the HBO dive. An expanded list of the 42 tentatively identified compounds with VIP scores >0.9 together with their ID scores, fold change between pre and post HBO, and p values, is provided in supplemental Table S3.

Many of the compounds listed in Table 2 are lipids or lipid-like molecules that are found in cell membranes and commonly serve to act as a membrane stabilizer. We speculate that the increased presence of many of these lipid-like molecules in the EBC of symptomatic subjects following the HBO dive may have resulted from tissue/cell damage in the lungs caused by the oxidative stress from reactive oxygen species overcoming antioxidative capacity leading to lipid peroxidation and the release of these compounds.

b) Comparison of Nitrox and HBO EBC profiles.—To explain the variations in EBC content between the nitrox dive (“chamber control exposure” breathing 30.6% O2 at 2 ATA for 6.5 h), and the high O2 dive (“chamber HBO exposure” using 100% O2 at 2 ATA for 6.5 h) we compared differences between three main classes: pre-dive, post nitrox dive sample (“post-N2O2”), and post HBO dive sample (“post-O2”). In this case, the same outlier samples were removed as explained in the previous section. The detected

targeted compounds did not show good classification abilities (AUC < 0.5, data not shown), but untargeted data provided better results (Table 3). The AUC was higher than 0.75 for all classes, with high values for both “post” dives (0.86 and 0.91 for nitrox and HBO, respectively). Specificities are good, with values around 0.85 for all the classes, allowing a good ability to reject a class from a sample that is not from that class. However, sensitivities are lower, reducing the ability to correctly classify samples from one specific class, especially with samples from “pre” dives.

A PLS-DA scores plot for this classification is presented in Figure 5a, where clear differences between Post-Nitrox and Post-O2 are observed. Although, visually, a good separation is appreciated between both post-dive samples, “pre” samples are less distinguishable and overlapped with the post-dive groups. The AUC are also presented in the ROC curves for each class (Figure 5b), reflecting the greater ability to differentiate “post-O2” samples from the rest. In this model, the “pre” sample for subject 8 was again clearly misclassified as a “post-O2” (see Subject 08 in Figure 5a). Predicted Y-values (Figure 5c) also show that the model can correctly distinguish individual “Post-N2O2” and “Post-O2” classes from the rest of the samples, with differences between groups being significant ($p < 0.05$). This model was built using 266 variables that were related to differences between the three classes. From this model, a final selection of 59 features were defined with VIP values greater than 1.

Finally, data were normalized based on the “pre” data using a matrix with both oxidative and nitrosative information. For that, a matrix containing 34 “post” samples was corrected using normalization by corresponding “pre” samples. 320 features were used to build a PLS-DA model (Figure 6). This model gave good classification abilities with AUCs of 0.99 (± 2%) and sensitivities and specificities of 0.93 (± 10%) and 0.94 (± 10%), respectively. A perfect differentiation between EBC samples collected after the “nitrox” and “HBO” dive was achieved.

Forty-nine features were defined by VIP values >0.9 and 20 (42%) were characterized with high ID score values (>65%). Table 4 shows putative identifications and molecular formulas, METLIN database-based score value (%), up- or down-regulation post-dive relative to normalized HBO conditions, and a short description of the compounds. Half of all the features (53%) were up-regulated, meaning their intensities increased after the 6.5h HBO exposure at 2 ATA relative to the nitrox exposure. Those features that are shown as down-regulated in Table 4 represent those compounds that were more highly expressed following the nitrox exposure compared to their level of expression following the HBO dive.

Tentative compounds that were found to be highly expressed (up-regulated) following the HBO exposure shown in Table 1 include grayanotoxin, a diterpenoid that has been detected in blood (30), and cardiogenol C (although both had low ID scores). Compounds identified in Table 4 that were more highly expressed following the HBO dive compared to the nitrox dive included other terpenoids, tripeptides, and several fatty acids. Interestingly, Table 1 shows that there were several different species of fatty acyls with high ID scores that showed decreased expression following the HBO dive. A common biomarker with high ID score noted in both Table 1 and Table 4 that was down-regulated following the HBO exposure is

related to alkane compounds with the chemical formula C6 H12. The functional/biological significance of this finding is unclear; however, it is possible that the reductions in this alkane in the EBC following the HBO exposure could be due to redox reactions involving free radical intermediates of oxygen.

One biomarker with high ID score that was more highly expressed following the nitrox dive compared to following the HBO exposure is (S)-2-propylpiperidine, an alkaloid that contains mostly basic nitrogen atoms. Again, the biological significance of this finding remains to be determined, with further studies needed to determine if this biomarker represents a functionally relevant characteristic of the difference in oxidative and/or nitrosative stress imparted by the different gas exposures.

When interpreting the data shown in Table 4 it should be kept in mind that while the duration of the dive and the total gas partial pressure were the same for the “control” nitrox dive as for the HBO dive, the nitrox dive will have resulted in a certain amount of decompression stress as a result of the uptake of nitrogen during the dive and its subsequent off-gassing following decompression to surface pressure (see footnote 3). Although not measured in the current study, it is possible that venous gas emboli (VGE) could have been generated in some subjects during and following decompression because of nitrogen off-gassing. Venous gas emboli can induce a variety of biological effects (31) through their interaction with blood (32, 33), incitement of epithelium damage, and microcirculatory impairment (34) that can result in an inflammatory response (35, 36). As venous gas emboli are filtered by the lungs it is possible that some of the biochemical products and metabolites resulting from the effects of the VGE are caried in the circulation and are subsequently reflected in the EBC. Consequently, the factors/biomarkers that distinguish the HBO dive from the nitrox dive in Table 4 likely reflect the effects of both the high level of hyperoxic stress following the HBO dive as well as potential effects of decompression stress following the nitrox dive.

Exposure to high partial pressures of nitrogen is known to generate microparticles (MPs) that contain elevated levels of IL-1β (37, 38). In addition, more recently Balestra et al., (2022) demonstrated MP generation following hyperoxic exposures. Interestingly, the number of blood-borne MPs was found to increase following 60 min exposures to 0.3 ATA, 1 ATA and 2.5 ATA of oxygen, but was decreased following a 60 min exposure to 1.4 ATA of oxygen (39). It is thus possible that some of the biomarkers shown in Table 1 and Table 4 may reflect basic elements or metabolites contained within or from these MPs as they pass through the circulation and into the lungs, however, further research is required to identify and confirm the compounds and their biochemical origin to solidify their use as a biomarker of hyperoxic or decompression stress.

A recent study conducted by de Jong et al., (2022) measured volatile organic compounds (VOCs) in the breath of healthy military personnel who underwent a hyperbaric oxygen treatment table 6 (TT6), with the aim of defining a VOC breath print indicative of subclinical PO2tox. While five VOCs, (i.e., isoprene, decane, nonane, nonanal, and dodecane), showed significant changes after the HBO exposure, only isoprene demonstrated a significant increase at 30 min after the TT6 exposure. It should be noted that none of

the subjects in this latter study reported signs or symptoms of PO2tox. In contrast, our study is unique in the literature in that over two thirds of our subjects reported signs and symptoms of PO2tox with one subject aborting the dive because of the severity of these symptoms. While our study and that of de Jong et al., (2022) analyzed different elements of the breath profile it is notable that both studies found several species of alkane compounds were down-regulated following the HBO exposure (40). This finding is in contrast with the general thought that the nonbranched or straight chain alkanes such as nonane or decane, are believed to be products of oxidative stress, and therefore should theoretically be increased because of action of ROS on polyunsaturated fatty acids in the lipid bilayers of cell membranes. Indeed, alkanes have been found to be increased in the breath of patients with pulmonary diseases such as asthma and chronic obstructive pulmonary disease compared to controls (41). Despite the unknown origin of the various alkanes, it appears that prolonged hyperbaric oxygen exposures up to the point of inducing the first signs and symptoms of PO2tox do not result in marked increases in these compounds (other than isoprene) in exhaled breath.

It should be born in mind that the compounds detected in exhaled breath condensate may change over time post-dive as the body's inflammatory reactions to the oxidative stress become more evident. Furthermore, a different pattern of breath compounds may be observed with more prolonged or stressful hyperbaric oxygen exposures than that employed in the present study. This may especially be the case if the hyperoxic stress progresses beyond the tracheobronchitis stage of PO2tox and induces significant diffuse alveolar damage like that seen with the onset of acute respiratory distress syndrome.

4. Conclusion

As far as we are aware, the current study is the first to describe potential biomarkers of hyperoxic stress in the exhaled breath condensate of subjects who reported signs and symptoms of PO2Tox following a prolonged HBO exposure. The PLS-DA models derived from untargeted EBC data showed good ability to differentiate between EBC samples collected before and after a 6.5h HBO exposure at 2 ATA, as well as between the HBO dive and a 2 ATA nitrox dive of the same duration but with a low level of hyperoxic stress. Furthermore, it was possible to identify those individuals who reported symptoms of pulmonary oxygen toxicity following the HBO dive from those who did not have symptoms based upon differences in their metabolomic EBC profile. The resulting classifications identified specific biomarkers that included human metabolites and fatty acyls and their derivatives from different metabolic pathways such as eicosanoids and oxylipins from cyclooxygenase (COX), lipogenase (LOX), cytochrome P450, and other non-enzymatic pathways that may explain metabolomic changes resulting from prolonged HBO exposure.

Supplementary Material

Refer to Web version on PubMed Central for supplementary material.

Acknowledgements

The Defense Health Program provided funding for this study through Joint Program Committee 5, Military Operational Medicine Research Program work unit F1604 and Restoral program work unit F2109. We wish to acknowledge the dive locker and staff at the Pressurized Submarine Escape Trainer, Naval Submarine School, Groton, CT for the use of their hyperbaric chamber facilities and the operational support that they provided in conducting the chamber dives for this study.

This work was supported by Naval Medical Logistical Command under prime contract number 62645-18-D-5049 and task/delivery order number N62645-18-F-0185 (Leidos, prime contractor). This work was also partially supported by: NIH NCATS awards 1U01TR004083 [CED], 1U18TR003795 [CED], 4U18TR003795 [CED] and UL1 TR001860 [CED]; NIH award UG3-OD023365 [CED]; NIH award 1P30ES023513-01A1 [CED]; University of California CITRIS and the Banatao Institute award 19-0092 [CED]; the Department of Veterans Affairs award I01 BX004965-01A1 [CED]; the University of California Tobacco-Related Disease Research Program award T31IR1614 [CED]. The contents of this manuscript are solely the responsibility of the authors and do not necessarily represent the official views of the funding agencies.

References

1. van Ooij PJ, Hollmann MW, van Hulst RA, Sterk PJ. Assessment of pulmonary oxygen toxicity: relevance to professional diving; a review. Respir Physiol Neurobiol. 2013;189(1):117–28. [PubMed: 23886638]
2. Undersea and Hyperbaric Medical Society (UHMS). Hyperbaric Oxygen Therapy Indications. 14th edition, Richard Moon Chair and editor, UHMS, North Palm Beach, FL. 2019.
3. Shykoff BE. Pulmonary effects of submerged oxygen breathing: 4-, 6-, and 8-hour dives at 140 kPa. Undersea Hyperb Med. 2005;32(5):351–61. [PubMed: 16457084]
4. Fothergill DM, Gertner J. Exhaled nitric oxide (NOexp) measurements as a noninvasive marker of pulmonary oxygen toxicity susceptibility in humans. Proceedings of the 35th Annual Scientific Meeting of the European Underwater and Baromedical Society and British Hyperbaric association Annual Meeting, The British Hyperbaric Association. 2009.
5. Aksenov AA, Zamuruyev KO, Pasamontes A, Brown JF, Schivo M, Foutouhi S, et al. Analytical methodologies for broad metabolite coverage of exhaled breath condensate. J Chromatogr B Analyt Technol Biomed Life Sci. 2017;1061–1062:17–25.
6. Davis C, Pleil J, Beauchamp J. Breathborne Biomarkers and the Human Volatilome: Elsevier Science; 2020.
7. Schmidt AJ, Borras E, Nguyen AP, Yeap D, Kenyon NJ, Davis CE. Portable exhaled breath condensate metabolomics for daily monitoring of adolescent asthma. J Breath Res. 2020;14(2):026001.
8. Zamuruyev KO, Aksenov AA, Pasamontes A, Brown JF, Pettit DR, Foutouhi S, et al. Human breath metabolomics using an optimized non-invasive exhaled breath condensate sampler. J Breath Res. 2016;11(1):016001.
9. Bajaj P, Ishmael FT. Exhaled Breath Condensates as a Source for Biomarkers for Characterization of Inflammatory Lung Diseases. Journal of Analytical Sciences, Methods and Instrumentation 2013;3(1).
10. Borras E, McCartney MM, Thompson CH, Meagher RJ, Kenyon NJ, Schivo M, et al. Exhaled breath biomarkers of influenza infection and influenza vaccination. J Breath Res. 2021;15(4).
11. Kubáň P, Foret F. Exhaled breath condensate: determination of non-volatile compounds and their potential for clinical diagnosis and monitoring. A review. Anal Chim Acta. 2013;805:1–18. [PubMed: 24296139]
12. Valenzuela OF, Encina MP. Design and evaluation of a device for collecting exhaled breath condensate. J Bras Pneumol. 2009;35(1):69–72. [PubMed: 19219333]
13. Gorrochategui E, Jaumot J, Lacorte S, Tauler R. Data analysis strategies for targeted and untargeted LC-MS metabolomic studies: Overview and workflow. TrAC Trends in Analytical Chemistry. 2016;82:425–42.
14. Sumner LW, Urbanczyk-Wochniak E, Broeckling CD. Metabolomics data analysis, visualization, and integration. Methods Mol Biol. 2007;406:409–36. [PubMed: 18287705]

15. Want E, Masson P. Processing and analysis of GC/LC-MS-based metabolomics data. Methods Mol Biol. 2011;708:277–98. [PubMed: 21207297]
16. Fan J, Upadhye S, Worster A. Understanding receiver operating characteristic (ROC) curves. Cjem. 2006;8(1):19–20. [PubMed: 17175625]
17. Cocchi M, Biancolillo A, Marini F. Chapter Ten - Chemometric Methods for Classification and Feature Selection. In: Jaumot J, Bedia C, Tauler R, editors. Comprehensive Analytical Chemistry. 82: Elsevier; 2018. p. 265–99.
18. Mansoor JK, Morrissey BM, Walby WF, Yoneda KY, Juarez M, Kajekar R, et al. L-Arginine Supplementation Enhances Exhaled NO, Breath Condensate VEGF, and Headache at 4342 m. High Alt Med Biol. 2005;6(4):289–300. [PubMed: 16351563]
19. Messina A, Nencioni S, Gervasi PG, Gotlinger KH, Schwartzman ML, Longo V. Molecular cloning and enzymatic characterization of sheep CYP2J. Xenobiotica. 2010;40(2):109–18. [PubMed: 20021200]
20. Carroll MA, Balazy M, Margiotta P, Huang DD, Falck JR, McGiff JC. Cytochrome P-450-dependent HETEs: profile of biological activity and stimulation by vasoactive peptides. Am J Physiol. 1996;271(4 Pt 2):R863–9.
21. Rahman M, Wright JT, Jr., Douglas JG. The role of the cytochrome P450-dependent metabolites of arachidonic acid in blood pressure regulation and renal function: a review. Am J Hypertens. 1997;10(3):356–65. [PubMed: 9056695]
22. Onodera T, Fukuhara A, Shin J, Hayakawa T, Otsuki M, Shimomura I. Eicosapentaenoic acid and 5-HEPE enhance macrophage-mediated Treg induction in mice. Sci Rep. 2017;7(1):4560. [PubMed: 28676689]
23. Jean-Louis T, Rockwell P, Figueiredo-Pereira ME. Prostaglandin J2 promotes O-GlcNAcylation raising APP processing by α- and β-secretases: relevance to Alzheimer's disease. Neurobiol Aging. 2018;62:130–45. [PubMed: 29149631]
24. Wright DH, Metters KM, Abramovitz M, Ford-Hutchinson AW. Characterization of the recombinant human prostanoid DP receptor and identification of L-644,698, a novel selective DP agonist. Br J Pharmacol. 1998;123(7):1317–24. [PubMed: 9579725]
25. Sawyer N, Cauchon E, Chateauneuf A, Cruz RP, Nicholson DW, Metters KM, et al. Molecular pharmacology of the human prostaglandin D2 receptor, CRTH2. Br J Pharmacol. 2002;137(8):1163–72. [PubMed: 12466225]
26. Mihaljević Z, Matić A, Stupin A, Frkanec R, Tavčar B, Kelava V, et al. Arachidonic Acid Metabolites of CYP450 Enzymes and HIF-1α Modulate Endothelium-Dependent Vasorelaxation in Sprague-Dawley Rats under Acute and Intermittent Hyperbaric Oxygenation. Int J Mol Sci. 2020;21(17).
27. Fang X, Kaduce TL, Weintraub NL, VanRollins M, Spector AA. Functional implications of a newly characterized pathway of 11,12-epoxyeicosatrienoic acid metabolism in arterial smooth muscle. Circ Res. 1996;79(4):784–93. [PubMed: 8831502]
28. Viswanathan S, Hammock BD, Newman JW, Meerarani P, Toborek M, Hennig B. Involvement of CYP 2C9 in mediating the proinflammatory effects of linoleic acid in vascular endothelial cells. J Am Coll Nutr. 2003;22(6):502–10. [PubMed: 14684755]
29. Hildreth K, Kodani SD, Hammock BD, Zhao L. Cytochrome P450-derived linoleic acid metabolites EpOMEs and DiHOMEs: a review of recent studies. J Nutr Biochem. 2020;86:108484.
30. Barupal DK, Fiehn O. Generating the Blood Exposome Database Using a Comprehensive Text Mining and Database Fusion Approach. 2019;127(9):097008.
31. Jauchem JR, Waligora JM, Conkin J, Horrigan DJ, Jr., Johnson PC, Jr. Blood biochemical factors in humans resistant and susceptible to formation of venous gas emboli during decompression. Eur J Appl Physiol Occup Physiol. 1986;55(1):68–73. [PubMed: 3698990]
32. Ackles K. Blood-bubble interaction in decompression sickness, Defence R&D Canada (DRDC), previously DCIEM, Canada 1973.
33. Ward CA, McCullough D, Fraser WD. Relation between complement activation and susceptibility to decompression sickness. Journal of applied physiology (Bethesda, Md : 1985). 1987;62(3):1160–6. [PubMed: 3494726]

34. Baz A, Abdel-Khalik SI. Effect of intravascular bubbles on perfusate flow and gas elimination rates following simulated decompression of a model tissue. Undersea Biomed Res. 1986;13(1):27–44. [PubMed: 3705248]

35. Bigley NJ, Perymon H, Bowman GC, Hull BE, Stills HF, Henderson RA. Inflammatory cytokines and cell adhesion molecules in a rat model of decompression sickness. J Interferon Cytokine Res. 2008;28(2):55–63. [PubMed: 18279101]

36. Marabotti C, Chiesa F, Scalzini A, Antonelli F, Lari R, Franchini C, et al. Cardiac and humoral changes induced by recreational scuba diving. Undersea Hyperb Med. 1999;26(3):151–8. [PubMed: 10485515]

37. Brett KD, Nugent NZ, Fraser NK, Bhopale VM, Yang M, Thom SR. Microparticle and interleukin-1β production with human simulated compressed air diving. Sci Rep. 2019;9(1):13320. [PubMed: 31527725]

38. Thom SR, Milovanova TN, Bogush M, Bhopale VM, Yang M, Bushmann K, et al. Microparticle production, neutrophil activation, and intravascular bubbles following open-water SCUBA diving. Journal of applied physiology (Bethesda, Md : 1985). 2012;112(8):1268–78. [PubMed: 22323646]

39. Balestra C, Arya AK, Leveque C, Virgili F, Germonpré P, Lambrechts K, et al. Varying Oxygen Partial Pressure Elicits Blood-Borne Microparticles Expressing Different Cell-Specific Proteins-Toward a Targeted Use of Oxygen? Int J Mol Sci. 2022;23(14).

40. de Jong FJM, Wingelaar TT, Brinkman P, van Ooij PAM, Maitland-van der Zee AH, Hollmann MW, et al. Pulmonary Oxygen Toxicity Through Exhaled Breath Markers After Hyperbaric Oxygen Treatment Table 6. Front Physiol. 2022;13:899568.

41. van de Kant KD, van der Sande LJ, Jöbsis Q, van Schayck OC, Dompeling E. Clinical use of exhaled volatile organic compounds in pulmonary diseases: a systematic review. Respir Res. 2012;13(1):117. [PubMed: 23259710]

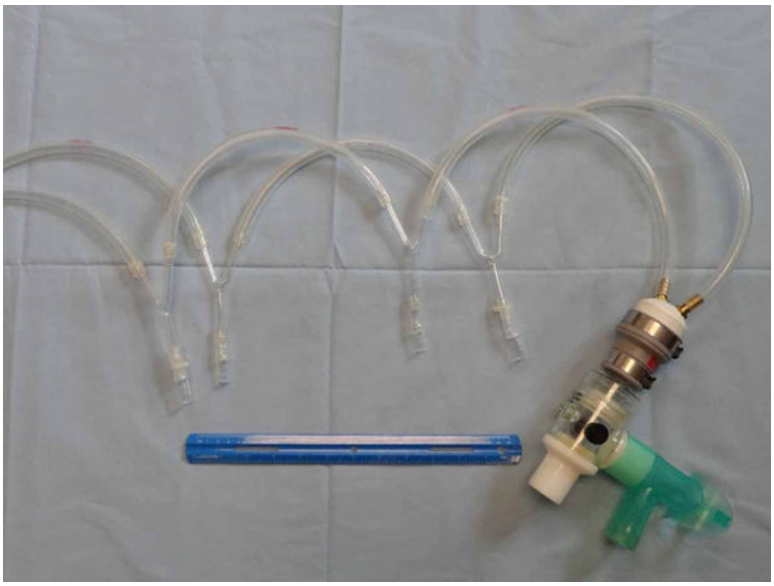

Figure 1.
EBC collection device based upon the design described in Valenzuela & Encina 2009 (12). The condensers were immersed in a cooler containing ice to condense the exhaled breath. Picture taken by the author.

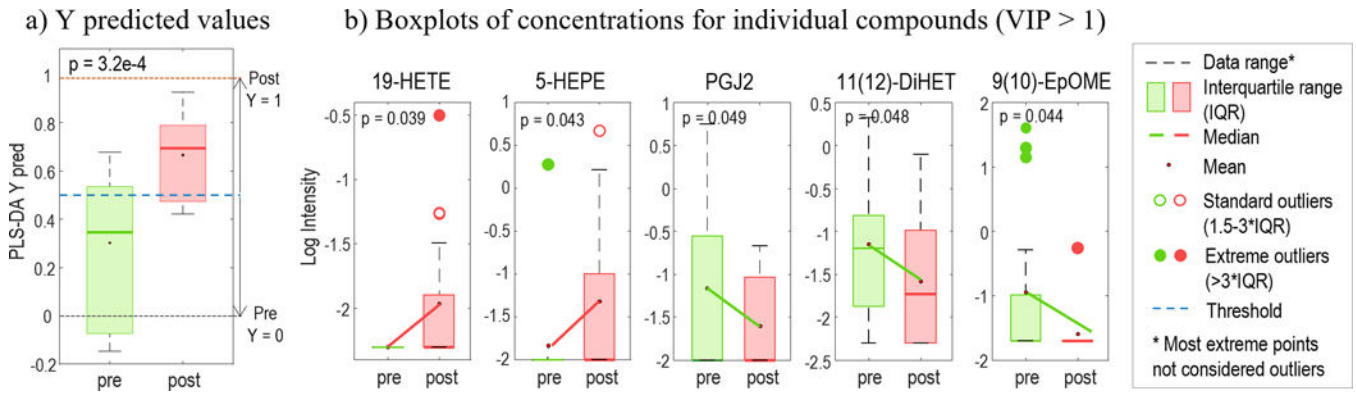

Figure 2.

Boxplots from targeted data presenting pre vs. post differences from subjects exposed to hyperbaric oxygen at 2 ATA for 6.5 hours. a) Y predicted values from PLS-DA model defining pre samples classified as pre (Y = 0) and post samples classified as post (Y = 1). b) Boxplots of concentrations from individual compounds that are characteristic from the defined PLS-DA model (VIP>1 and $p<0.05$).

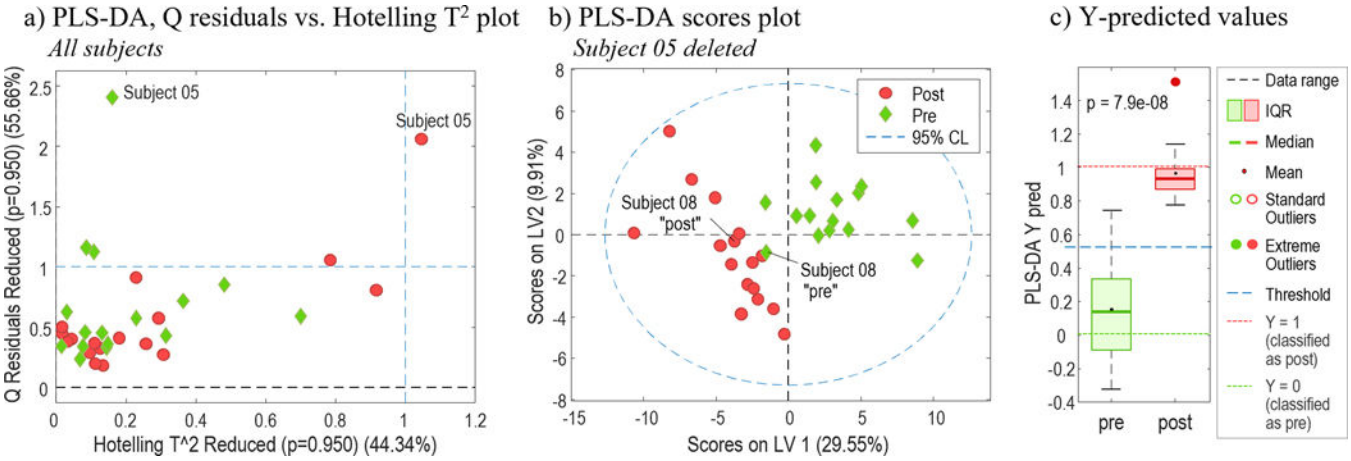

Figure 3.

Untargeted data PLS-DA model for pre vs. post differences from subjects exposed to 2 ATA of HBO for 6.5 hours. a) Q residual and Hotelling T^2 plot for the PLS-DA model using all subjects' data, b) PLS-DA scores plot built deleting outlier sample (Subject 05); c) Y predicted values defining pre samples classified as pre (Y = 0) and post samples classified as post (Y = 1).

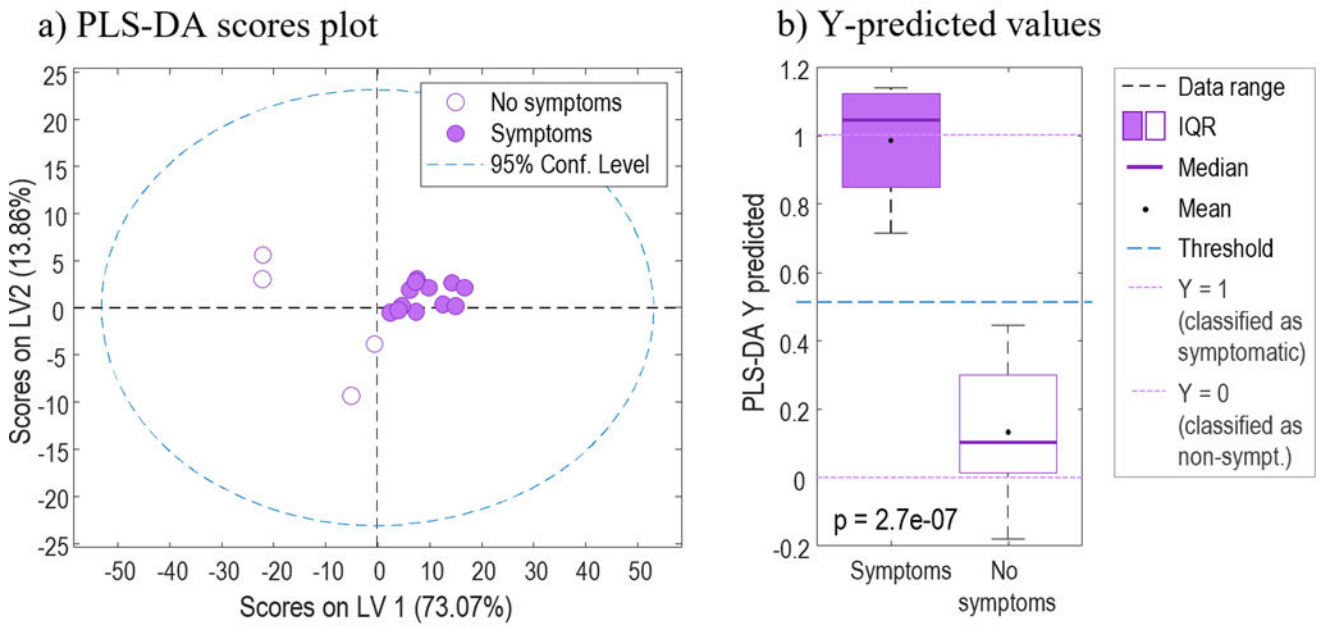

Figure 4.

Untargeted PLS-DA model of the normalized EBC data for the HBO dive that differentiates those subjects who reported pulmonary oxygen toxicity symptoms following the dive from those without symptoms. A) PLS-DA scores plot, and B) Y predicted values defining HBO samples showing symptoms (Y=1) and showing no symptoms (Y=0) after the HBO dive.

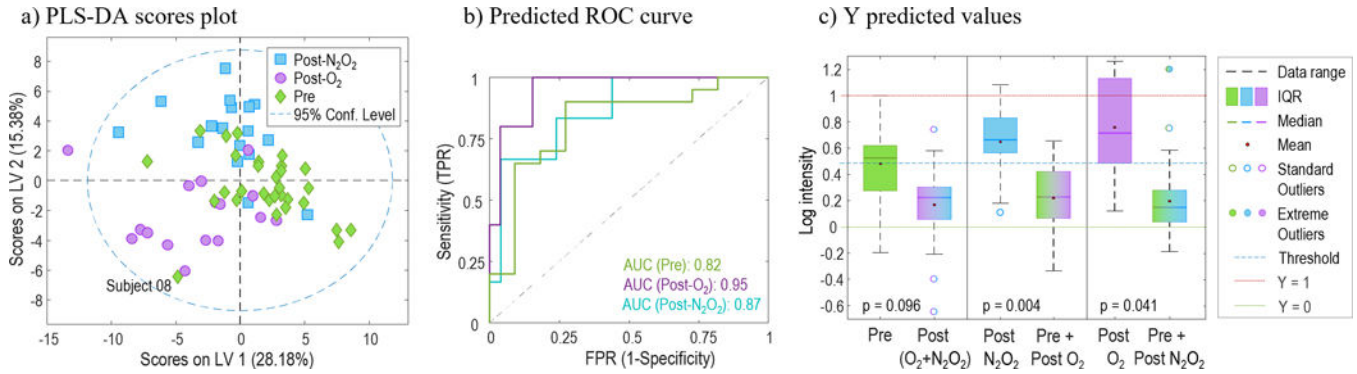

Figure 5.

Untargeted data PLS-DA model for “pre”, “post-N_2O_2”, and “post-O_2” differences. A) PLS-DA scores plot presenting 3 groups of classes; b) Predicted ROC curve values; and c) Y predicted values defining individual classes classified as is (Y = 0) and rest of the classes (Y = 1).

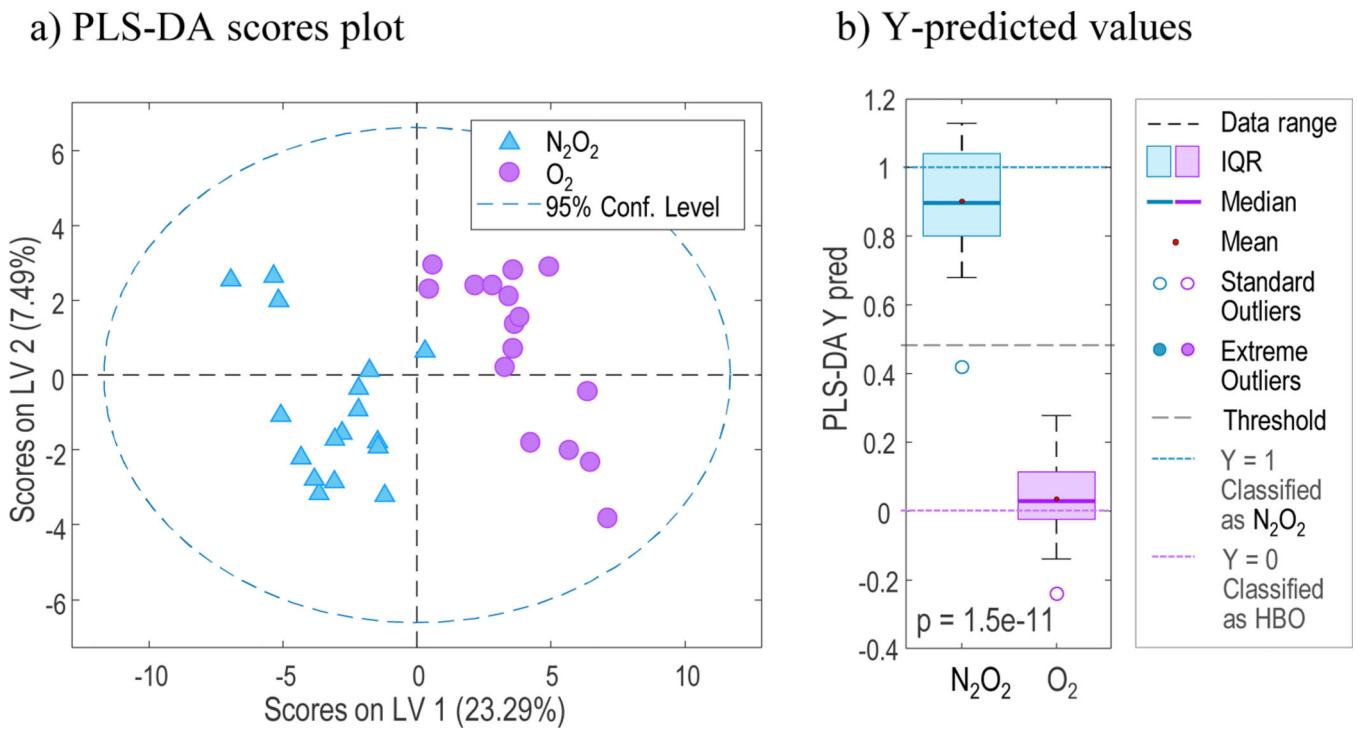

Figure 6.

Untargeted data PLS-DA model to differentiate Nitrox (N_2O_2) and HBO (O_2) exposures after data normalization. A) PLS-DA scores plot; b) Y predicted values defining samples from "N_2O_2" class (Y = 1) and from "O_2" class (Y = 0).

Table 1.

Characterization of main biomarkers that explain EBC differences between pre and post hyperbaric oxygen exposure

Comp.	Molecular formula	Compound ID	ID score (%)	Post HBO dive regulation	Description
1	C11 H20 O	10-Undecen-2-one / (1R,2R)-1,2,7,7-Tetramethylbicyclo[2.2.1]heptan-2-ol / 9-Undecenal / 3-Methyl-3E-decen-2-one / 2-Methylisoborneol	86.70	up	Metabolites
2	C13 H16 N4 O2	Cardiogenol C	68.10	up	Cardiomyogenic
3	C22 H36 O7	Grayanotoxin I	66.80	up	Diterpenoids
4	C5 H11 N	Piperidine	87.50	up	Metabolites
5	C6 H12	2E-Hexene / Methylcyclopentane / Cyclohexane	96.7*	down	Alkanes
6	C29 H32 O17	Tricetin 4'-methyl ether 7-apiosyl-(1->2)-(6''-acetylglucoside) / Tricin 7-rhamnosyl-(1->2)-galacturonide / Luteolin 7-(6'''-acetylsophoroside) / Kaempferol 3-(6''-acetylglucosyl)-(1->3)-galactoside / Luteolin 7-(6'''-acetylallosyl-(1->2)-glucoside)	95.6*	down	Metabolites
7	C14 H26 O5	3-Hydroxy-tetradecanedioic acid	95.3*	down	Fatty acyls
8	C20 H32 O4	8S,15S-DiHETE(Z,E,E,E) / 5S,15S-DiHETE / 11-HpETE	94.3*	down	Fatty acyls
9	C10 H14 N2	Phenylpiperazine / Trimethyl-2-propenylpyrazine / (±)-Nicotine / Anabasine	93.7*	down	Metabolites
10	C25 H37 N O4	Salmeterol / 15(R)-17-phenyl trinor Prostaglandin F2α ethyl amide	87.40	down	Benzenoids
11	C6 H8 O3	2-Hydroxy-cis-hex-2,4-dienoate	87.10	down	Fatty acyls
12	C8 H10 O5	Endothall / Erinapyrone C	85.50	down	Metabolites
13	C16 H18 N2 O3	Pilosine / Levcromakalim / Cromakalim	85.00	down	Azoles
14	C10 H20 N6 O4	Gly Arg Gly	83.50	down	Tripeptides
15	C19 H27 N O4	alpha-Eucaine	83.50	down	Drug metabolites
16	C5 H8 O2	3-Methyl-2-butenoic acid / Angelic acid / 2-Ethylacrylic acid / b-Penteic acid	83.40	down	Fatty acyls
17	C5 H10 O2	Pivalic acid / Valeric acid / Isovaleric acid / Methyl isobutanate / 3-Hydroxy-3-methylbutan-2-one	83.20	down	Metabolites
18	C32 H43 N5 O5	Dihydroergocryptine	83.20	down	Drug metabolite
19	C9 H15 N O2	Homoarecoline / Piperidione / Aceclidine	77.90	down	Metabolites
20	C16 H30 O5	9-hydroxy-hexadecan-1,16-dioic acid / 10-hydroxy-hexadecan-1,16-dioic acid	75.90	down	Fatty acyls
21	C10 H14 N2 O2	Laccarin / Pilocarpidine / 6-Hydroxypseudooxynicotine	71.30	down	Metabolites
22	C8 H14 O4	Suberic acid / Ethyladipic acid / Dimethyl adipate / Dimethoxane / Diethy succinate	71.10	down	Metabolites
23	C17 H10 O	Benzanthrone	70.90	down	Metabolites
24	C11 H14 O4	3,4-Dihydroxyphenylvaleric acid / 2'-Hydroxy-4',6'-dimethoxy-3'-methylacetophenone / 2-Methoxy-4-(4-methyl-1,3-dioxolan-2-yl)phenol / 2-Methoxy-3-(4-methoxyphenyl)propanoic acid	69.90	down	Metabolites
25	C18 H16 O3	6-hydroxy-7E,9E-Octadecadiene-11,13,15,17-tetraynoic acid / (2-Isopropyl-1-benzofuran-3-yl)(4-hydroxyphenyl)methanone / 2-(4-	68.70	down	Metabolites

Comp.	Molecular formula	Compound ID	ID score (%)	Post HBO dive regulation	Description
		Methoxyphenethyl)chromone / Ipriflavone / Phenprocoumon			
26	C5 H13 N	2-Methylbutylamine / 3-Methylbutylamine	68.40	down	Monoalkylamines

*(indicates > 90% ID score).

For an expanded list of the biomarkers see supplemental Table S2.

Table 2.

Characterization of main biomarkers that explain EBC differences between symptomatic and non-symptomatic subjects after the HBO dive

Comp.	Molecular formula	Compound ID	ID score (%)	Symptom-regulation	Description
1	C26 H37 N O6	17-phenyl trinor Prostaglandin E2 serinol amide / Militarinone A	93.2 *	up	Metabolites/lipids
2	C16 H23 N5 O	Tegaserod	88.40	up	Drug (indole derivative)
3	C29 H42 O5	Minabeolide-8 / 17,23-Epoxy-29-hydroxy-27-norlanost-8-ene-3,15,24-trione / (3beta,17alpha,23S)-17,23-Epoxy-3,29-dihydroxy-27-norlanosta-7,9(11)-diene-15,24-dione	78.30	up	Anti-inflammatory metabolite / Triterpenoids
4	C35 H52 O8	Phorbol 12-tiglate 13-decanoate	68.20	up	Phorbol Esters
5	C8 H11 N	2,4-xylidine / N-Ethylaniline / Phenylethylamine	82.90	up	Metabolites
6	C16 H28 N4 O8	Glu Glu Lys	98.0 *	up	Peptides
7	C31 H48 O4	26-Methyl nigranoate / 1-Hydroxyprevitamin D3 diacetate / (22R)-1α,22,25-trihydroxy-26,27-dimethyl-23,24-tetradehydro-24a,24b-dihomo-20-epivitamin D3 / (22R)-1α,22,25-trihydroxy-26,27-dimethyl-23,24-tetradehydro-24a,24b-dihomo-20-epicholecalciferol	93.9 *	up	Lipids/Triterpenoids
8	C21 H44 O7 P	PC(13:0/0:0)	77.20	up	Lipids
9	C13 H18 O7	Methylarbutin / 3-Hydroxy-4,6-heptadiyne-1-yl 1-glucoside / Salicin	85.50	up	Metabolites
10	C27 H36 O6	Lucidenolactone / Lucidenic acid F	65.5	up	Triterpenoids
11	C15 H20 N2 O6	Val-Val-OH / Abu-Leu-OH / Ile-Abu-OH	79.50	up	Peptides
12	C10 H18 N2 O2	Slaframine	85.40	up	Metabolite (indolizidines)
13	C24 H40 O7 S	3-Sulfodeoxycholic acid / Ursodeoxycholic acid 3-sulfate / Chenodeoxycholic acid sulfate	96.5 *	up	Deoxycholic Acid/ analogs and derivatives
14	C18 H22 N2 O4	Methyl (E)-4-((3aS)-6-methoxy-1-methyl-5-oxo-2,3,5,8a-tetrahydropyrrolo[2,3-b]indol-3a(1H)-yl)-2-methylbut-2-enoate	75.40	up	Unknown
15	C12 H24 O6	Hexyl glucoside	66.4	up	Metabolite (Fatty acyl glycoside)
16	C22 H24 O9	Agehoustin B / Isosakuranetin 7-O-rhamnoside / Pinostrobin 5-O-glucoside / Strobopinin 7-galactoside	79.50	up	Lipids / Flavonoids
17	C17 H23 N3 O6	Phe Ala Glu / Pro Tyr Ser	83.30	up	Peptides
18	C7 H12 O2	3-Methyl-2E-hexenoic acid / Pimelic dialdehyde / Heptenoic acid / Ethyl tiglate	84.30	up	Fatty acyls

* (ID score > 90%).

Regulation: up-regulation represents those features that were more highly expressed by symptomatic subjects after the HBO exposure; down-regulation represents those features more highly expressed by non-symptomatic subjects following the HBO exposure. For a complete list of the biomarkers see supplemental Table S3.

Table 3.

Untargeted PLS-DA classification results for the effect of dive conditions. AUC = area under the curve.

	AUC	Sensitivity	Specificity
Class 1 (Pre)	0.76 (± 8%)	0.68 (± 13%)	0.86 (± 12%)
Class 2 (Post-Nitrox)	0.86 (± 10%)	0.71 (± 30%)	0.85 (± 9%)
Class 3 (Post-O_2)	0.91 (± 5%)	0.77 (± 22%)	0.84 (± 10%)

Table 4.

Characterization of main biomarkers that explain EBC differences between Nitrox and HBO dives

Comp.	Molecular formula	Compound ID	ID score (%)	Regulation	Description
1	C8 H17 N	(S)-2-Propylpiperidine	94.5 *	down	Alkaloids
2	C31 H34 O17	Kaempferol 3-(4’’,6’’-diacetylglucoside)-7-rhamnoside / Apigenin 7-(4’’,6’’-diacetylalloside)-4’-alloside	88.02	down	Flavonoids
3	C6 H12	Cyclohexane / Methylcyclopentane / 2E-Hexene	87.25	down	Alkanes
4	C13 H20 O3	13-Oxo-9,11-tridecadienoic acid / (8alpha,10beta,11beta)-3-Hydroxy-4,15-dinor-1(5)-xanthen-12,8-olide / Octyl 2-furoate / Furfuryl octanoate / 3-Methylbutyl 2-furanbutanoate	86.79	down	Metabolites
5	C10 H12 O	2,4,6-Trimethylbenzaldehyde / 3,4,5-Trimethylbenzaldehyde / 2,4-dimethylacetophenone / 2-(4-methylphenyl)propanal	86.43	down	Metabolites
6	C4 H8 O	Butanal / Buten-1-ol / 1,2-Epoxibutane	85.84	down	Metabolites
7	C13 H20 N2 O	Prilocaine	85.32	down	Drug metabolite
8	C10 H14 O4	(2E,4E)-2,7-Dimethyl-2,4-octadienedioic acid / 1-(3,4-Dimethoxyphenyl)ethane-1,2-diol / 5-(3E-Pentenyl)tetrahydro-2-oxo-3-furancarboxylic acid / 3-(4-Hydroxy-3-methoxyphenyl)-1,2-propanediol	82.08	down	Fatty acyls
9	C8 H14 O4	Suberic acid / Ethyladipic acid / Dimethyl adipate / Dimethoxane / Diethy succinate	79.52	down	Metabolites
10	C5 H13 N	2-Methylbutylamine / 3-Methylbutylamine	66.74	down	Monoalkylamines
11	C15 H22 O2	Germacrene A acid / b-Santalic acid	94.5 *	up	Sesquiterpenoids
12	C13 H25 N7 O5	Gly Gln Arg / Gly Arg Gln / Arg Gly Gln	93.4 *	up	Peptides
13	C10 H16 O4	3,7-Dimethyl-2E-octene-1,8-dioic acid / (±)-Camphoric acid / (1R,2R,3S,1’R)-Nepetalinic acid / Matsutakic acid A	87.23	up	Metabolites
14	C16 H22 O6	3-O-Benzyl-4,5-O-(1-methylethyldiene)-b-D-fructopyranose / Tetranor-PGJM / Tetranor-PGAM	84.13	up	Fatty acyls
15	C13 H16 N4 O2	Cardiogenol C	82.18	up	Cardiomyogenic
16	C21 H26 N2 O3	Corynanthine	78.56	up	Steroids
17	C19 H22 O8	Hydroxyvernolide / 3,4-DHPEA-EA / Gibberellin / 2-(3,4-Dihydroxyphenylethyl)-6-epi-elenaiate	72.27	up	Metabolites
18	C21 H21 F N2 O	YM-53601	65.15	up	Squalene derivative
19	C8 H12 O2	4Z,7-octadienoic acid / C8:2n-1,4	65.40	up	Fatty acyls
20	C9 H16 O3	n-butyrl n-valeric acid / 4-n-valeryl butyric acid / 3-caproyl propionic acid / 8-oxo-nonanoic acid	65.00	up	Fatty acyls

* (ID score > 90%).

Regulation: up-regulation represents those features that were more highly expressed following the HBO exposure; down-regulation represents those features more highly expressed following the nitrox exposure. For an expanded list of the biomarkers see supplemental Table S4.